

Electrochemical properties of carbon nanofiber web as an electrode for supercapacitor prepared by electrospinning

C. Kim and K. S. Yang

Citation: [Appl. Phys. Lett.](#) **83**, 1216 (2003); doi: 10.1063/1.1599963

View online: <http://dx.doi.org/10.1063/1.1599963>

View Table of Contents: <http://apl.aip.org/resource/1/APPLAB/v83/i6>

Published by the [American Institute of Physics](#).

Additional information on Appl. Phys. Lett.

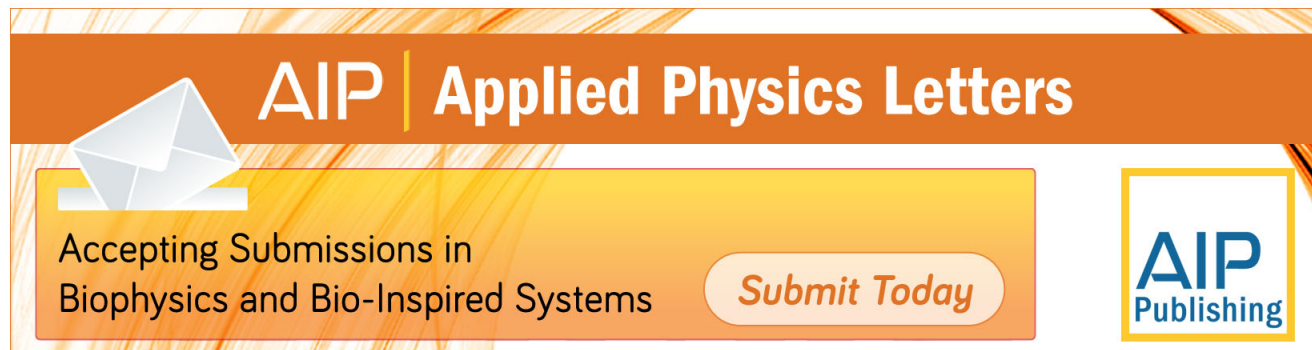
Journal Homepage: <http://apl.aip.org/>

Journal Information: http://apl.aip.org/about/about_the_journal

Top downloads: http://apl.aip.org/features/most_downloaded

Information for Authors: <http://apl.aip.org/authors>

ADVERTISEMENT

The advertisement banner features a background of orange and yellow diagonal stripes. At the top, the "AIP Applied Physics Letters" logo is displayed in white. Below the logo, on the left, is a white envelope icon. To its right, the text "Accepting Submissions in Biophysics and Bio-Inspired Systems" is written in black. Further right, a white button with the text "Submit Today" in orange is shown. On the far right, the "AIP Publishing" logo is displayed in blue and yellow.

Electrochemical properties of carbon nanofiber web as an electrode for supercapacitor prepared by electrospinning

C. Kim and K. S. Yang^{a)}

Faculty of Applied Chemical Engineering, Chonnam National University, 300 Youngbong-dong, Buk-gu, Gwangju 500-757, Korea

(Received 12 March 2003; accepted 6 June 2003)

Poly(acrylonitrile) solutions in dimethylformamide were electrospun to be webs consisting of 300 nm ultrafine fibers. The webs were oxidatively stabilized and activated by steam resulting in activated carbon nanofibers (ACNFs). The specific surface area of the ACNF activated at 700 °C was the highest but mesopore volume fraction of that was lowest. On the other hand, the ACNFs activated at 800 °C showed opposite trends to those activated at 700 °C. The high specific surface area, mainly due to the micropores, introduced maximum specific capacitance at low current density (173 F/g at 10 mA/g). The elevated volume fraction of mesopores gave maximum specific capacitance at high current density (120 F/g at 1000 mA/g). The behavior is explained on the basis of ion mobility in the pores. © 2003 American Institute of Physics. [DOI: 10.1063/1.1599963]

Electrospinning is a method to produce nanofibers by using an electrostatically repulsive force and an electric field between two electrodes, by applying high voltage to a polymer solution or a melt, so that it can make a web of nanofibers.^{1–5} Generally, the fiber diameter electrospun is dependent on the viscosity and electric conductivity of the polymeric fluids, and the applied voltage. The nonwoven web obtained from the electrospinning was used to produce activated carbon nanofibers (ACNFs), through stabilization, carbonization-activation processes. The activated carbon nanofiber produced has a high specific surface area from shallow pores size. The shallow pores could be formed due to the nanosize in fiber diameters through the activation resulting in enhanced specific capacitance at elevated current density.

Another advantage of the electrospinning is that it can be used to produce a web structure. When used as an electrode, it does not need a second processing step adding a binder and an electric conductor such as carbon black. Therefore, the webs from electrospinning have important advantages such as an ease of handling, an increase in the energy density due to large specific surface area, an improvement of the conductivity due to increased density of the contact points, and low cost of preparations of the electrodes.

However, the structural characterizations and their effects on electrochemical properties of poly(acrylonitrile) (PAN)-based ACNFs have not yet been reported. In this letter, we demonstrate the potentiality of the PAN-based ACNF web as an electrode material with enhanced capacitance and electrical properties of the supercapacitor.

PAN (10 wt %) was dissolved in dimethylformamide. The solution was spun into fiber web through the capillary positively charged using an electrospinning apparatus at dc 10–25 kV (HYP-303D power supply, Han Young Co., Korea) The negative electrode was connected to drum winder collecting the webs. The details were reported elsewhere.⁶

The electrospun fiber web was stabilized by heating at

1 °C/min up to 280 °C and holding for 1 h under air flow. The stabilized nanofiber webs were heated at a rate of 5 °C/min up to 700, 750, and 800 °C and activated for 30 min by supplying 30 vol. % of steam in a carrier gas of N₂. The fiber surface and diameter were analyzed by scanning electron microscopy (SEM) (Hitachi, S-4100, Japan). Specific surface areas and pore size distributions of the ACNF webs were evaluated by using the Brunauer–Emmett–Teller equation, after preheating the ACNFs at 150 °C for 2 h to eliminate water adsorbed.

A unit cell was prepared with a pair of the ACNF web separated by a filter paper. The electrical double layer capacitor (EDLC) performances were tested in a 30 wt % KOH aqueous solution. Cyclic voltammetry (CV) of the unit cell was performed in the potential range of 0–0.9 V at a scan rate of 10 mV/s. The discharge capacitance (*C*) of the electrodes in EDLC were calculated on the basis of

$$C = 2(i \times \Delta t) / (W \times \Delta V), \quad (1)$$

where *i* is the current, Δt is the discharging time from 0.54 to 0.45 V (about 60%–50% of the initial voltage), ΔV is the voltage variation in the time range measured, and *W* is the weight of the two electrodes.

Figure 1 shows scanning electron micrographs the ACNFs of the activated fibers with diameter from 200 to 400 nm. The effects of variations of pore structures on the adsorption properties of ACNFs were studied by isotherms of nitrogen adsorption at 77 K. The specific surface area decreased with an increase in activation temperature. This trend is opposite to those of other ACFs produced by traditional fiber spinning techniques. This behavior could be explained by taking into account the mesopore volume fraction. The mesopore volume fraction increased from 36% (at 700 °C) to 62% (at 800 °C) with variations in activation temperature, though there was no significant change in average pore diameter as shown in Table I. The behaviors would imply that more mesopores were formed through unifications of the micropores at elevated activation temperatures.

^{a)}Electronic mail: ksyang@chonnam.chonnam.ac.kr

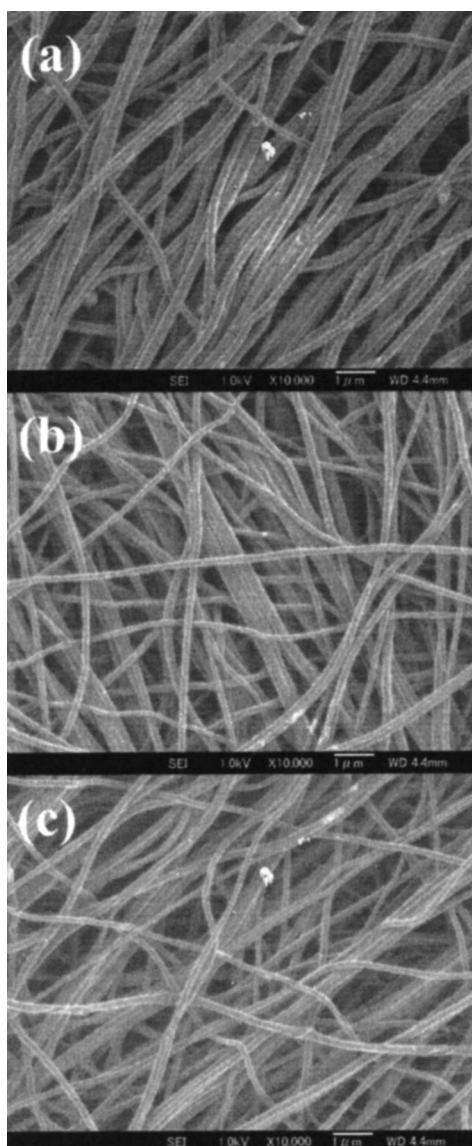


FIG. 1. SEM micrographs of PAN-based ACNF web as a function of activated temperatures (a) 700, (b) 750, and (c) 800 °C.

Figure 2 shows the specific capacitance as a function of the discharge current density of ACNFs electrodes. In general, the specific capacitance decreases from the peak point with an increase in the deviation from current density of 10 mA/g. The behaviors would be attributed to the dissipation of some portion of the supplied current at a certain rate along the direction of normal to the graphene layers from the compact double layer with the mechanism of an intrinsic semiconductor.⁸ When the current density is lower, the portion of dissipation would be enlarged. Too large currents may reduce the accessibility of ions through the micropores and thus reduce the specific capacitance.⁷

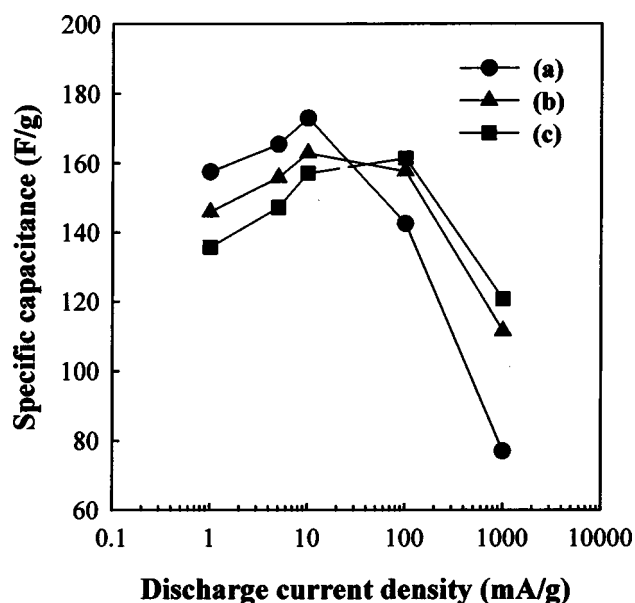


FIG. 2. Dependence of specific capacitances on the discharge current density for PAN-based ACNF web at various activation temperatures (a) 700, (b) 750, and (c) 800 °C.

The maximum capacitance was obtained as 175 F/g from the electrode with the largest surface area [Fig. 2(a)]. Below the current density of 10 mA/g, higher the specific surface area, higher the specific capacitance resulted. On the other hand, above 10 mA/g, the lower surface area, the higher capacitance was resulted. This behavior can be explained by the accessibility of the ions on the pore surface. The electrode activated at 700 °C exhibits highest specific surface area and lowest fraction of mesopore volume fraction under the experimental condition. Whereas, the electrode activated at 800 °C showed the lowest surface area but the highest mesopore volume fraction. The ions solvated by water molecules in the mesopores would respond more quickly than those in the micropores at a higher current density above 10 mA/g in this case. Consequently, the electrode with higher fraction of mesopores would have a higher specific capacitance at higher current density. Thus, at a lower current density, the capacitance is predominantly dependent on the specific surface area, while at high current density it depends mostly on the mesopore volume fraction. For example, at a lower activation temperature of 700 °C, the specific capacitance at 1000 mA/g dropped by about 55% in comparison with that at 10 mA/g, as shown in Fig. 2(a). However, for the electrode activated at 800 °C, the capacitance reduced by only about 18% at the same current density [Fig. 2(c)]. The high capacitance at high current density would be a practical importance for capacitor applications.

Figure 3(a) shows CV of ACNF electrodes at a 10 mV/s

TABLE I. Various properties of ACNFs.

Sample	Burn off (%)	BET surface area (m ² /g)	Average pore diameter (Å)	Pore volume fraction (%)		Total pore volume (cm ³ /g)
				Micropore	Mesopore	
PAN700	50	1230	31	64	36	0.55
PAN750	60	1100	30	58	42	0.46
PAN800	70	850	32	38	62	0.37

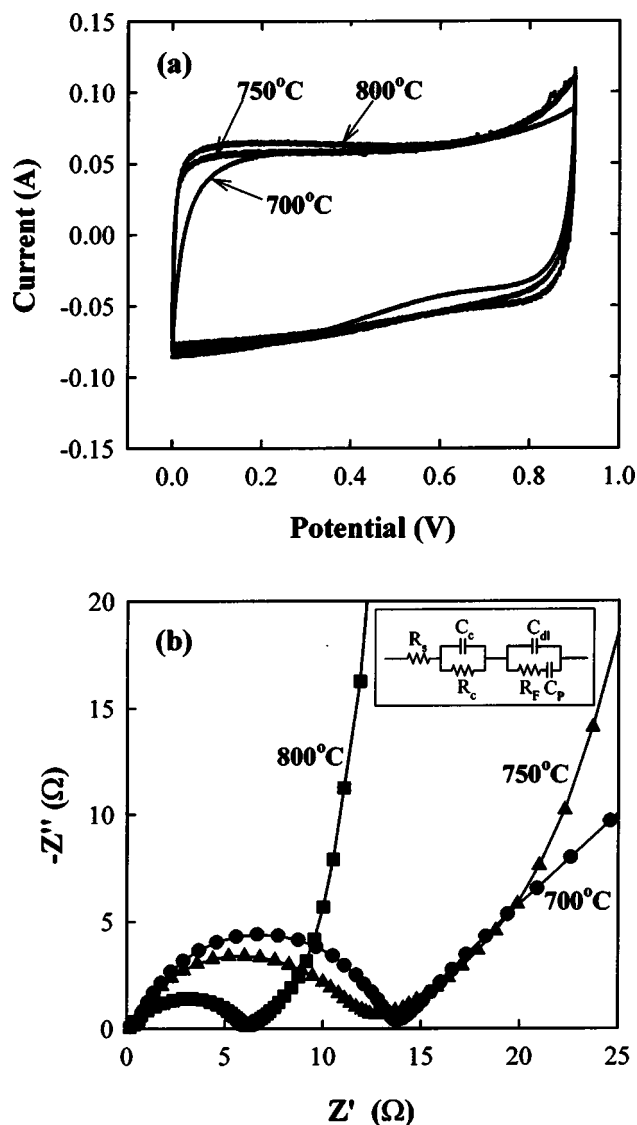


FIG. 3. Electrochemical properties of the supercapacitor using the ACNF electrodes. (a) Cyclic voltammograms of ACNF electrodes in 30 wt % KOH electrolyte at potential sweep rate of 10 mV/s. (b) Impedance Nyquist plots of an EDLC (ac signal level, 20 mV; frequency range, 1 mHz–1 MHz). Inset shows the equivalent circuit representation.

scan rate. When the activation temperature was increased from 700 to 800 °C, the CV curve approached to a rectangular shape, indicating the smallest equivalent series resistance in the ACNF electrode and a reduction in hindrance of motion of the ions in the pores.

The electrochemical behavior of the electrodes could be more clearly understood by ac impedance measurement. The

complex impedance spectra for various samples were shown in Fig. 3(b). Taking into account the pseudocapacitance attributed to redox process of the oxygen containing functional groups,⁸ the equivalent circuit model of the EDLC will be as the inset of Fig. 3(b).⁹ Where R_s is the ohmic solution resistance, which is constant for a given electrolyte; C_{dl} , the double layer capacitance; R_F , the Faradic resistance; C_p , the pseudocapacitance; C_c and R_c , capacitance and resistance arisen between the fibers as well as between fabric and collecting plate for the electrical connections. The overall impedance, Z , of the equivalent circuit can be written as

$$Z = R_s + \frac{R_c}{j\omega R_c C_c} + \frac{1}{j\omega C_{dl} + \frac{j\omega C_p}{j\omega R_F C_p + 1}} \quad (2)$$

Clearly, Eq. (2) represents the locus of a semicircle that intercepts the $R_e(Z)$ axis at R_s and $R_s + R_c$ in the Nyquist plot [Fig. 3(b)]. If it was considered that the resistances of electrolyte and the contact resistances are identical in all the samples, a decrease in $(R_s + R_c)$ value indicates a decrease of the ACNF electrode resistance. Figure 3(b) shows that ACNF-electrode resistance decreased with an increase in activation temperature. The ideal capacitance will give rise to a straight line along the imaginary axis (Z'') at lower frequency. In a capacitor with a series resistance, this line has a finite slope representing the mass transfer resistivity of the electrolyte within the pore of the electrode, as represented by Warburg impedance. With increasing activation temperature, the slope of the impedance representing mass transfer approached to an ideally straight line [Fig. 3(b)] implying the enhanced accessibility of the ions and/or the possible contributions of pseudocapacitance.

This work was supported by Korea Research Foundation Grant No. (KRF-2002-002-D00103).

¹J. Doshi and D. H. Reneker, *J. Electrochem. Soc.* **35**, 151 (1995).

²C. J. Buchko, L. C. Chen, Y. Shen, and D. C. Martin, *Polymer* **40**, 7397 (1999).

³D. H. Reneker and I. Chun, *Nanotechnology* **7**, 216 (1996).

⁴J. S. Kim and D. H. Reneker, *Polymer Eng. Sci.* **39**, 849 (1999).

⁵M. Bognitzki, W. Czado, T. Frese, A. Schaper, M. Hellwig, M. Steinhart, A. Greiner, and J. H. Wendorff, *Adv. Mater. (Weinheim, Ger.)* **13**, 70 (2001).

⁶C. Kim and K. S. Yang, *Carbon Science* **3**, 211 (2002) (in Korean).

⁷K. H. An, W. S. Kim, Y. S. Park, J. M. Moon, D. J. Bae, S. C. Lim, Y. S. Lee, and Y. H. Lee, *Adv. Funct. Mater.* **11**, 387 (2001).

⁸D. Qu, *J. Power Sources* **109**, 403 (2002).

⁹Y. R. Nian and H. Teng, *J. Electrochem. Soc.* **149**, A1008 (2002).